

1 **Novel para-aortic cardiac assistance using a pre-stretched dielectric elastomer actuator**

2 **Authors:** Silje Ekroll Jahren^{1,2*}, Thomas Martinez^{1*}, Armando Walter¹, Francesco Clavica^{1,2}, Paul
3 Philipp Heinisch^{3,4}, Eric Buffle⁵, Markus M Luedi⁶, Jurgen Hörer⁴, Dominik Obrist², Thierry Carrel⁷,
4 Yoan Civet¹, Yves Perriard¹

5 * These two authors contributed equally to this work

6 **Affiliations:**

7 ¹ Integrated Actuators Laboratory (LAI), École polytechnique fédérale de Lausanne (EPFL),
8 Neuchâtel, Switzerland

9 ² ARTORG Center for Biomedical Engineering Research, University of Bern, Bern, Switzerland

10 ³ Department of Congenital and Pediatric Heart Surgery, German Heart Center Munich, Technical
11 University of Munich, Munich, Germany.

12 ⁴ Division of Congenital and Pediatric Heart Surgery, University Hospital of Munich, Ludwig-
13 Maximilians-University, Munich, Germany.

14 ⁵ Department of Cardiology, Bern University Hospital Inselspital, University of Bern, Bern,
15 Switzerland

16 ⁶ Department of Anaesthesiology, Bern University Hospital Inselspital, University of Bern, Bern,
17 Switzerland

18 ⁷ Department of Cardiac Surgery, University of Zurich, Zurich, Switzerland

19
20 The manuscript was accepted for EACTS 2023 annual meeting.

21
22 **Word count** : 4738 words

23
24 **Corresponding Author:** Silje Ekroll Jahren, Freiburgstrasse 3, 3010, Bern, Switzerland.
25 +41 31 632 08 17, silje.jahren@unibe.ch

1 **ABSTRACT**

2 **Objectives**

3 We propose an evolution of a dielectric elastomer actuator based cardiac assist device that acts
4 as a counterpulsation system. We introduce a new pre-stretched actuator and implant the device
5 in a graft bypass between the ascending and descending aorta to redirect all blood through the
6 device (ascending aorta clamped). The objective was to evaluate the influence of these changes
7 on the assistance provided to the heart.
8

9 **Methods**

10 The novel para-aortic device and the new implantation technique were tested in-vivo in 5 pigs.
11 We monitored the pressure and flow in the aorta as well as the pressure-volume characteristics
12 of the left-ventricle. Different activation timings were tested to identify the optimal device
13 actuation.
14

15 **Results**

16 The proposed device helps reducing the end-diastolic pressure in the aorta by up to $13 \pm 4.0\%$ as
17 well as the peak systolic pressure by up to $16 \pm 3.6\%$. The early diastolic pressure was also
18 increased up to $10 \pm 3.5\%$. With different activation we also showed that the device could increase
19 or decrease the stroke volume.
20

21 **Conclusions**

22 The new setup and the novel para-aortic device presented here helped improve cardiac
23 assistance compared to previous studies. Moreover, we revealed a new way to assist the heart
24 by actuating the device at different starting time to modify the left ventricular stroke volume and
25 stroke work.
26

27
28 **Keywords:** Dielectric Elastomer Actuator, Cardiac Assist Device, Counterpulsation, *in vivo*
29 experiment
30

31 **List of acronyms and abbreviations:**

32 HF: Heart Failure

33 VAD: Ventricular Assist Device

34 ACP: Aortic Counterpulsation

35 DEA: Dielectric Elastomer Actuator

36 HV: High Voltage

37 PV: Pressure Volume

38 PS: Phase Shift

39 PLV: Pressure in the Left Ventricle

40 Pasc: Aortic pressure
41
42
43

1 INTRODUCTION

2 Heart failure (HF) is a condition characterized by a reduced ability of the heart to pump blood.
3 Sixty-four million people were estimated to suffer from HF worldwide in 2017 and, due to its high
4 prevalence, HF is considered a global pandemic. The costs projections associated with HF, for the
5 year 2030, suggest that approximately 70 billion dollars will be spent for HF in USA alone. For
6 severe heart failure, heart transplant is considered the gold standard. Cardiac assist devices has
7 been introduced as bridge to transplantation because of the shortage of heart donors. More
8 recently, the interest of these devices has shifted towards a destination strategy[1,2].
9 Nevertheless, cardiac assist devices as destination therapies are still unmet clinical needs [3].

10
11 Currently, Ventricular Assist Devices (VADs) with rotary pumps are the most common cardiac
12 assist solutions [4]. They generate a constant flow and are characterized by high durability.
13 However, due to the high shear stress generated by the rotating components on the blood,
14 current VADs can cause haemolysis and thrombosis which force patients to follow
15 anticoagulation treatment for the whole duration of the cardiac support [5]. On the contrary,
16 assist devices based on aortic-counterpulsation (ACP) do not require anticoagulation treatment
17 [6] and can help preserving (or even augment) the aortic pulsatile flow [7]. There exist several
18 types of ACP devices which are named based on their location within the aorta. The ACP working
19 principle is similar in all devices as they are designed to reduce the afterload during systole, and
20 increase the coronary flow during diastole [8]. The ACP devices are still short-term solutions to
21 bridge other options (e.g. VADs or patient recovery) in high-risk patients. This is mainly because
22 of the high risk of ischemia [9] associated with the 'large' ACP transcatheter pneumatic
23 drivelines.

24
25 Dielectric elastomer actuators (DEAs) emerge as a compelling alternative to existing assist
26 devices, distinguished by their softness compared to rigid VADs and their sole reliance on
27 electrical activation, compared to existing pneumatic ACP devices. These advantages could
28 enable an implantable device and long-term cardiac support. DEAs consist of a hyperelastic
29 dielectric membrane sandwiched between two compliant electrodes. Applying high-voltage
30 between the electrodes generates a Maxwell pressure that compresses the dielectric elastomers
31 in the thickness dimension, enabling expansion in the other directions [10]. In our previous work
32 [11], we already demonstrated the potential of our approach by showing the effects of the DEA
33 as a cardiac assist device in porcine animal models. At the beginning of systole, the DEA is
34 activated and can store more blood thus decreasing the pressure in the ascending aorta. This
35 decrease in pressure continues while the device is active. When the aortic valve closes, the DEA
36 is deactivated, and the stored blood is released leading to an increase of pressure in the aorta.
37 The effect is similar to the effect of intra-aortic balloon pumps.

38
39 In (14), the DEA was implanted in the descending aorta, far from the aortic valve. Consequently,
40 the pressure waves generated by the DEA underwent significant damping and energy-losses
41 before reaching the aortic valve [12]. Moreover, only a fraction of the total blood flow passed
42 through the DEA (due to the supra-aortic vessels upstream of the DEA). The main reason which
43 prevented DEA implantation in ascending aorta was the limited space, due to the shorter porcine

1 ascending aorta (approximately 4 cm versus 8 cm of human aorta) [13]. The goal of the current
2 study is to demonstrate that a pre-stretched soft DEA can support the heart by lowering the end-
3 diastolic pressure and increasing early aortic diastolic pressure compared to previous versions
4 [11]. Pre-stretching the DEAs is an easy and inexpensive technique that allows to increase the
5 maximum electric field the DEA can sustain and limit its breakdown [14,15]. This pre-stretch,
6 results into a more stable and more performant DEA. In addition, by measuring the pressure-
7 volume characteristics of the left ventricle, we want to show the effect of our assist device on
8 the stroke volume and stroke work of the heart. Finally, we aim to demonstrate the pertinence
9 of the new implantation technique to reproduce conditions closer to the human ones for the
10 cardiac assist device.
11

12 **MATERIALS AND METHODS**

13 **Ethical statement**

14 This experiment presented in this paper was approved by the Commission of Animal
15 Experimentation of the Canton of Bern, Switzerland (Approval number BE14/2021).
16

17 **A pre-stretched dielectric elastomer actuator for cardiac assist device**

18 The DEA cardiac assist device is based on a tubular dielectric elastomer actuator. The initial tube
19 has a total length of 40 mm, a diameter of 25 mm and an overall thickness of around 500 μm and
20 is made of Elastosil 2030 (Wacker Chemie AG, Munich, Germany), a silicone elastomer. Compared
21 to previous works, in this study, the DEA is pre-stretched axially and maintained in this position
22 with an external housing. We were thus able to increase its length up to 60 mm, i.e. a 1.5 times
23 pre-stretch. The full housing of the DEA as shown in **Figure 1** A and B allows also to have a
24 different diameter between the aorta and the DEA. By increasing the diameter of the DEA, the
25 activation and deactivation of the device generate a higher displacement of blood volume and
26 increases the effect on the cardiovascular system.

27 The pressure-volume characteristics of the DEA characterize the behaviour of the actuator and
28 allow to estimate the volume displacement and the energy provided by the DEA during *in vivo*
29 experiments. They were obtained through *in vitro* tests at different actuation voltages. The
30 experimental testbench consists of a pneumatic system composed of a piston and a motor
31 connected to the device and coupled to a pressure sensor (Baumer PBMN-25B12, Frauenfeld,
32 Switzerland) [11,16]. At different actuation voltages, the motor is moved to increase the pressure
33 in the device while the displacement is measured with a 2D laser sensor (Gocator 2030, LMI
34 Technologies, Vancouver, Canada) yielding the pressure-volume characteristics at constant
35 voltage.
36

37 **Implantation of the device and measurements**

38 An acute porcine model was used to test our device *in vivo* in n=5 Edelschwein pigs ranging from
39 50 to 70 kg. The complete anaesthesia process for the pigs is described in the supplementary
40 materials. For the *in vivo* experiments, a new surgery protocol has been developed. The thoracic

1 cavity was accessed with an extended left sided thoracotomy (Hemi-clam-shell incision) and the
2 pericardium was opened after administration of intravenous heparin. To implant the DEA, the
3 aorta was partially clamped by a Satinsky clamp, first in the ascending aorta (close to the first
4 branch of the aortic arch) and then in the descending aorta at the level of the diaphragm. Dacron-
5 Grafts (12-18mm Gelweave, Vascutek Ltd., Inchinnan, United Kingdom) were sutured as end-to-
6 side anastomosis to the ascending and the descending aorta and cut in half (**Figure 1 C**). The DEA
7 was embedded in between the two remaining Dacron-Grafts to allow exchange of the devices.
8 After DEA implantation, the Satinsky clamps were removed. During the experimental testing of
9 the DEA device an aortic cross clamp was placed just below the truncus brachiocephalicus to
10 allow blood flow to be directed exclusively through the DEA device into the descending aorta. In
11 case of exchange of the DEA device the aortic cross clamp was temporally removed. With this
12 new configuration, the whole blood exiting the left ventricle passed through the graft and the
13 DEA, followed by the descending aorta where the flow splits in two streams. One stream goes
14 through the normal path going down the descending aorta and the other goes back up the
15 descending thoracic aorta to supply the aortic arch and the aortic branches.

16 All the sensors are shown in **Figure 1 D**. Blood flow was measured with ultrasonic flow probes
17 (Confidence, Transonic Systems, Inc., Ithaca, NY, USA) on each side of the connection between
18 the graft and descending aorta to measure the total blood flow. Two water-filled pressure
19 catheters (Xtrans, CODAN Pvb Critical Care GmbH, Forstinning, Germany) were inserted near
20 these flow probes. Two additional pressure sensors were positioned in the DEA and in the
21 ascending aorta as close as possible to the aortic valve. Finally, a pressure-volume catheter
22 (Millar, ADInstruments, Houston, USA) was inserted in the left ventricle through the apex. The
23 heart rate was controlled with a pacemaker. The pacemaker also acted as a trigger to synchronize
24 the activation of the device with the heart.

25 All data were recorded through two acquisition consoles (Powerlab, ADInstruments, Houston,
26 USA) and the DEA was actuating by a HV amplifier (Trek 20/20C, Advanced Energy, Denver, USA).
27 controlled by a compactDAQ (National Instruments, Austin, USA) acquisition card as shown in
28 **Figure 1 E**.

29 **Testing protocol**

30 The testing protocol was identical to the one presented for the previous animal experiment [11].
31 First, we defined a reference time for the start of activation. This time was set to have the
32 decompression pressure wave, created by the activation of the DEA, arriving at the aortic valve
33 at opening. Similarly, the end of activation is chosen to be in synchronisation with the aortic valve
34 closure. This leads to an earlier activation compared to the opening of the valve because of the
35 propagation time of the pressure wave from the location in the graft to the aortic valve. The
36 synchronization between the pacemaker, the opening of the valve and the actuation of the DEA
37 is described in more depth in [11]. We then defined two protocols based on this reference time
38 as shown in **Figure 2 A** and **B**. In the first protocol **A**, the activation profile of the DEA remained
39 fixed, and we changed the start of activation by phase shifting it through the heart cycle in
40 percent of the heart cycle duration. With this protocol, we obtain insight into the influence of the
41 activation of the DEA throughout the heart cycle. In the second protocol **B**, we focused on fine
42 tuning the activation of the DEA. The first protocol allowed to define the starting time that results
43 in the optimal assistance to the heart. From this starting point, we then slightly change the start

1 and end of activation to find the overall best configurations that maximize the assistance to the
2 heart.

3
4 For each DEA, the two protocols were performed at a given voltage. We proceeded with
5 incremental voltage steps: if the DEA sustained the experiment, we increased the voltage and
6 carried out the two protocols at this higher voltage. We continued this increase until the DEA
7 suffered electrical breakdown.
8

9 **Statistical Analysis**

10 Cardiac parameters were recorded during baseline (60 heart cycles before and 60 heart cycles
11 after device-actuated period) and during actuation of the device (60 heart cycles). Only 40
12 consecutive heart cycles, 20 baseline and 20 device-actuated (either with baseline cycles before
13 actuation followed by the first cycles of actuation or with the last cycles of actuation followed by
14 the first baseline cycles after actuation), for each device protocol were analysed using MATLAB
15 (MathWorks, Natick, US) to limit the effect of irregular events such as arrhythmia or nonstable
16 hemodynamic conditions in the analysis. The 20+20 heart cycles were consecutive, and for each
17 of the cycles pressure, flow, and volume parameters were calculated. Additionally, the mean
18 values and standard deviations for the baseline (20 cycles) and device-actuated cycles (20 cycles)
19 were calculated for each parameter. To compare actuated cycles with baseline among all animals
20 and all devices, the mean values were normalized to baseline for each observation (20+20 cycles)
21 by calculating the change compared to baseline in percentage as $100 * (\text{mean of actuated cycles} - \text{mean of baseline cycles}) / (\text{mean of baseline cycles})$. For each device protocol, the normalized
22 observations were grouped in range of actuation timings (phase shifts) and the Wilcoxon signed-
23 rank test (signrank in MATLAB) was performed to compare the device-actuated cycles with the
24 baseline cycles for all DEAs and all animals. The same test was used to compare the different
25 groups of actuation timing. To compare the different animals, we performed the Kruskal-Wallis
26 test (kruskalwallis in MATLAB), and if significant, we performed a multiple comparison
27 (multcompare in MATLAB) to test which animals were significantly different. A p-value below
28 0.05 was considered significant.
29
30

31 **RESULTS**

32 All the pigs were implanted with the pre-stretched DEA. At baseline, the 5 included pigs had aortic
33 pressures in the range of 51.3-118.0 mmHg (mean: 88.3 ± 11.0 mmHg) and 24.6-78.3 mmHg
34 (mean: 46.7 ± 13.8 mmHg) systolic and diastolic pressure, respectively. The cardiac output ranged
35 from 1.2-5.7 L/min (mean: 3.1 ± 0.9 L/min). Supplementary **Table S1** shows an overview of the
36 used DEAs, the actuation voltages, and the performed protocols for each animal. All recordings
37 performed in Animal 2 were excluded from the analysis due to poor data quality (e.g., signal
38 noise), arrhythmic events or nonstable hemodynamic condition of the animal. Additionally, the
39 pressure-volume catheter signals were difficult to measure (due to e.g., motion artifacts and
40 pressure sensor touching the ventricular wall) leading to only a few recordings in Animal 5 with
41 an acceptable signal quality. No device-related adverse events were observed in any animal, and
42 no animal died during surgery. Across the animals, a significant difference of actuation response

1 was observed ($p < 0.05$). However, across the animals with comparable actuation voltage (animal
 2 3 and 4) no statistical significance was observed ($p > 0.05$). The different response of animal 1 and
 3 5 compared to animal 3 and 4 can be attributed to the lower actuation voltage (animal 1) and to
 4 the loss of performance of the DEAs due to device extensive usage (animal 5) leading to lower
 5 responses to actuation. The statistical analysis across the animals can be seen in the
 6 supplementary material **Figure S1**.

7 **Improved assistance to the heart: up to 16 %**

8 The best DEA-assistance results are achieved with counterpulsation (start of actuation around opening of the
 9 aortic valve and end of activation around the closure of the aortic valve). **Figure 3** show all results from the two
 10 protocols (A: phase shifts, B: fine-tuning) and all animals, and how the different parameters are affected by the
 11 DEA actuation timing.

12 **Table 1** shows the mean values and the standard deviations of the same parameters. The p-values for significant
 13 differences compared to baseline within each group and the number of recordings are presented in **Table S2** in the
 14 supplementary material. The results from protocol A (**Figure 3** A,C,E,G), show that the optimal start of activation
 15 lies between 90% and 10% delay thus defining the study area for protocol B (fine tuning). Compared to baseline,
 16 the end-diastolic pressure (**Figure 3** A, B) decreases by up to $13 \pm 4.0\%$ (start of actuation before aortic valve
 17 opening: -30% to 0% of heart cycle ($p < 0.05$), range: 2-10% decrease,

18 **Table 1**), the mean early aortic diastolic pressure (**Figure 3** C, D) increases by up to $10 \pm 3.5\%$ (end of actuation
 19 around aortic valve closure: -20% to 10% of heart cycle ($p < 0.05$), range: 3-5% increase,

20 **Table 1**), the maximum systolic pressure (**Figure 3** E,F) decreases by up to $16 \pm 3.6\%$ (start of actuation around
 21 aortic valve opening: -10% to 30% of heart cycle ($p < 0.05$), range: 2-7% decrease,

22 **Table 1**), and the mean systolic left ventricular pressure (**Figure 3** G,H) decreases by up to $5 \pm 3.8\%$ (start of
 23 actuation around aortic valve opening: -10% to 10% of heart cycle ($p < 0.05$), range: 1-3% decrease,

24 **Table 1**). The different groups of DEA actuation timing were found to be significantly different
 25 ($p < 0.05$) for both protocols (see supplementary material **Figure S2** for more detail).

26 **Overall best results for the aortic pressure parameters**

27 **Figure 4** shows examples of the overall best results observed during all experiments
 28 (interindividual) performed in this study for the ascending aortic pressure parameters. **Figure 4**
 29 A shows the case (Animal 3, DEA 4, 6kV, protocol B, start and end actuation timing: -4%, -3%)
 30 with the relative largest reductions in maximum systolic aortic pressure and end-diastolic
 31 pressure, and **Figure 4** B shows the relative largest increase in mean early aortic diastolic pressure
 32 (Animal 3, DEA 4, 6kV, protocol B, start and end actuation timing: -5%, -11%). **Figure 4** C shows
 33 the relative best overall assistance of the same three parameters observed simultaneously
 34 (Animal 4, DEA 5, 6kV, protocol B, start and end actuation timing: -8%, 0%).

35 **Influence of actuation timing on the pressure-volume characteristics of the left ventricle**

36 The pressure-volume characteristics of the left ventricle is influenced by the DEA actuation
 37 timing. **Figure 5** shows the pressure-volume characteristics during counterpulsation (A) and for
 38 three different phase shifts (actuation timings) (B) observed in animal 5 (Note: due to limited
 39 recordings with working pressure-volume measurements these results are single observations).
 40 During counterpulsation the pressure-volume loops shifts to the left (**Figure 5** A), the mean
 41 systolic left ventricular pressure decreases (2%) and the stroke volume increases (4%). For the
 42 phase shifts (**Figure 5** B), an actuation at the beginning of systole (phase shift 5%) lowers the
 43 mean systolic left ventricular pressure (5%) without altering the stroke volume and thereby

1 reduces the stroke work of the ventricle (4%). An actuation during end of systole (phase shift
2 25%) sucks more blood out of the ventricle just before aortic valve closure and increases the
3 stroke volume (6%) with a small decrease in **mean** systolic left ventricular pressure (3%), leading
4 to a larger stroke work. A deactivation during end of systole (phase shift 75%), however, pushes
5 blood towards the ventricle while the aortic valve is still open. This reduces the stroke volume
6 significantly (15%) without altering the **mean** systolic left ventricular pressure leading to a
7 significant decrease in stroke work (14%). In this case, the device hinders the work of the heart.

8 **Pre-stretching the DEA increases the energy provided to the cardiovascular system**

9 The energy provided by the DEA during the *in vivo* experiments were estimated from the *in vivo*
10 pressure measurements and through comparison with the *in vitro* tests performed at static
11 pressure levels. In **Figure 6 A**, we compare the estimated energy of the pre-stretched DEA to the
12 previous DEA design without pre-stretch [11] at similar pressure levels *in vivo*. The here reported
13 pre-stretched DEA supplies 29.5 mJ against 5.75 mJ for the previous DEA design without pre-
14 stretch with a voltage lower than before, 6 kV against 7 kV. In **Figure 6 B**, we represent the
15 recording with the (interindividual) largest estimated energy provided during the current *in vivo*
16 experiments (animal 3, DEA 4, protocol A, 6 kV, start and end actuation timing: 2.3 %,-1.8 %). In
17 this case, the difference of pressure inside the DEA between activation and deactivation is almost
18 50 mmHg leading to energy as high as 82.3 mJ. Moreover, at 90 mmHg, the volume of blood
19 displaced during deactivation is very high climbing up to 28 mL, almost ten times more than with
20 the previous design.

21 **DISCUSSION**

22 We presented a new design for the dielectric elastomer actuator (DEA) and a new implantation
23 technique was introduced with a graft bypass between the ascending aorta and the descending
24 aorta and with the DEA implanted in it. This new setup was tested *in vivo* in a porcine model (n =
25 4) while monitoring hemodynamic parameters such as the aortic and left-ventricle pressures,
26 blood flow and volume of the left-ventricle.

27 **Better assistance to the heart with pre-stretched DEA**

28 The new pre-stretched DEA design improved the energy provided to the heart and the volume of
29 blood displaced during activation and deactivation of the device. Additionally, the voltage
30 required to activate the DEA was reduced. In this *in vivo* work, we show improvement of the
31 assistance to the heart compared to our previous DEA design without pre-stretch [11]. For the
32 best cases shown here, the end-diastolic pressure and peak systolic pressure in the aorta were
33 reduced 2.5 and 6.5 times more compared to the reduction observed with our previous design,
34 and the early diastolic aortic pressure increased 5 times more compared to the previous design.
35 Moreover, during this experiment, we could exploit some of the data from the pressure-volume
36 catheter inserted in the left ventricle to showcase the influence of the DEA on the pressure-
37 volume characteristics. We found out that for the same activation timing that led to the
38 optimized results presented before, the work of the left ventricle was reduced due to the
39 lowering of the pressure (afterload). Additionally, a small increase in stroke volume was
40 observed. This is comparable to the effects reported during intra-aortic balloon support. [17–19].
41 However, by choosing a different start for the activation different effects can be achieved:
42 increase or reduction in left ventricular pressure, stroke volume and stroke work. We must add
43

1 that although these effects are very significant on the displayed results, they lack statistical
2 evidence as the measurement was not exploitable for many of the tested DEAs due to bad
3 positioning of the PV catheter. Nonetheless, the actuation timing could still be tuned to fit the
4 desired effect for the patient.

5
6 This constitutes a notable difference compared to other counterpulsation systems especially
7 intra-aortic balloon pumps. The DEA is never obstructing the blood flow and thus can be actuated
8 in different parts of the heart cycle. On the contrary activation is limited to only diastole for intra-
9 aortic balloon pump. Furthermore, in terms of assistance, the new setup presented here allows
10 to reach the levels provided by intra-aortic balloon pumps regarding the decrease in end-diastolic
11 pressure. In [20], Kolyva et al. reported reduction in end-diastolic pressure up to 13.7 % and
12 similar results were presented in [21] with 13.9 % reduction for intra-aortic balloon pump. The
13 authors also reported an increase of the peak diastolic aortic pressure of 26.7 %. For para-aortic
14 balloon pumps, decrease in end-diastolic pressure of 34.7 % and increase of 39.2 % of the peak
15 diastolic aortic pressure are demonstrated [21]. However, for this latter device, the inflation can
16 deflect the flow of blood from its natural path as the balloon is implanted outside of the aorta.
17 The typical values of volume inflation in these systems range from 30 to 50 cm³ for intra-aortic
18 balloon pumps and 40 cm³ for para-aortic balloon in [21] allowing more assistance to the heart
19 than with our device. We showed that the maximum displacement of volume, for our device, was
20 28 cm³ but the typical range goes from 10 to 25 cm³. These results depend greatly on the
21 hemodynamic parameters and, more importantly, on the pressure range at which the DEA is
22 working. For clinical application where the pressure range might be higher, our actuator could
23 provide more volume displacement and surpass typical IABP assistance results.

24 25 **Strengths and weaknesses of the new surgery configuration**

26 In the new surgical configuration, all blood ejected from the heart passes through the graft and
27 the DEA. In addition, the DEA is located closer to the aortic valve. Both these changes should
28 improve the assistance to the cardiovascular system: i) they ensure a better synchronization of
29 the device with the cardiac cycle due to its proximity to the aortic valve, ii) the counterpulsation
30 efficiency and blood volume displacement are maximized because the flow in the actuator is
31 increased and the pulse propagation in other arteries is minimized, and iii) we can expect the
32 blood flow in the coronary arteries to be maximized [22,23]. However, adding a rigid graft bypass
33 in the blood flow, increases the afterload (resistance) of the left ventricle and potentially the
34 workload compared to the native configuration. Furthermore, the presented surgery remains
35 very invasive and complex, although it allows more easy replacement of defective devices (by
36 reopening the clamp in the ascending aorta and clamp the graft during exchange). This
37 experimental surgery, however, remains a testing setup that allows to emulate conditions closer
38 to the final application, i.e., implantation in the human ascending aorta, but does not represent
39 the final clinical application.

40 41 **Perspectives**

42 The presented results show a significant improvement compared to previous designs and
43 showcase the interest of this solution for future clinical application. The proposed DEA based
44 cardiac assist device only require electric stimulation and research is currently ongoing to develop

1 transcutaneous wireless power transfer in order to have a fully implanted device (without
2 drivelines passing through the skin) [24]. Furthermore, some aspects of the systems are being
3 refined to be more adapted to clinical applications. We are currently working on reducing the
4 invasiveness of the surgery by wrapping the DEA around the aorta (extra-aortic) and on
5 synchronization of the actuation with electrocardiogram (ECG) electrodes. The latter especially
6 could be beneficial in chronic experiments.

7 8 **CONCLUSION**

9 In this work, we propose a new design of a DEA based cardiac assist device. The new pre-
10 stretched DEA was able to supply more energy and displace more volume of blood than the
11 previous design without pre-stretch. The new design combined with the surgical implantation of
12 the device helped improving the assistance to the heart. Furthermore, we demonstrated a new
13 operating mode to assist the heart with the same device as when changing the activation timing,
14 the activation of the device can increase the stroke volume or reduce the stroke work of the left-
15 ventricle.

16
17 **Acknowledgments:** We would like to thank the experimental surgery facility team of University
18 of Bern (Dainela Casoni, Kay Nettelbeck, Luisana Garcia, Angela Wicki, MariaFrancesca Petrucci).

19
20 **Funding:** This study was supported by the Werner Siemens Stiftung

21
22 **Data Availability Statement:** All data are available upon request to the corresponding author.

23
24 **Author Contributions:** T.M., A.W., and Y.C. designed the device. A.W. fabricated the device. T.M.
25 and A.W. characterized the actuators. S.E.J. and F.C. designed the acquisition and sensor setup.
26 S.E.J., F.C., P.P.H., and YC wrote the ethical approval. P.P.H., J.H. and Y.C. designed the new
27 surgical procedure. S.E.J., T.M., A.W., F.C., P.P.H., E.B. and Y.C. conducted the porcine studies.
28 S.E.J., T.M., F.C., P.P.H., E.B., M.M.L., J.H., D.O., T.C., Y.C., and Y.P. designed the research. S.E.J. and
29 T.M. analysed the data. S.E.J., T.M., F.C. and Y.C. wrote the paper. S.E.J., T.M., A.W., F.C., P.P.H.,
30 E.B., M.M.L., J.H., D.O., T.C., Y.C., and Y.P. reviewed the paper.

31
32 The authors have declared that no competing interests exist.

33 34 **References and Notes**

- 35 [1] Loor G, Gonzalez-Stawinski G. Pulsatile vs. continuous flow in ventricular assist device
36 therapy. *Best Pract Res Clin Anaesthesiol* 2012;26:105–15.
37 <https://doi.org/10.1016/j.bpa.2012.03.004>.
- 38 [2] Bornoff J, Najjar A, Fresiello L, Finocchiaro T, Perkins IL, Gill H, et al. Fluid–structure
39 interaction modelling of a positive-displacement Total Artificial Heart. *Sci Rep*
40 2023;13:5734. <https://doi.org/10.1038/s41598-023-32141-2>.

- 1 [3] Tatum R, Briasoulis A, Tchantchaleishvili V, Massey HT. Evaluation of donor heart for
2 transplantation. *Heart Fail Rev* 2022;27:1819–27. [https://doi.org/10.1007/s10741-021-](https://doi.org/10.1007/s10741-021-10178-7)
3 [10178-7](https://doi.org/10.1007/s10741-021-10178-7).
- 4 [4] Ganapathi MD AM, Salerno MD CT, Mokadam MD NA. Left Ventricular Assist Devices:
5 Description of Available Technologies. *Textbook of Transplantation and Mechanical*
6 *Support for End-Stage Heart and Lung Disease*, John Wiley & Sons, Ltd; 2023, p. 691–705.
7 <https://doi.org/10.1002/9781119633884.ch50>.
- 8 [5] Malone G, Abdelsayed G, Bligh F, Al Qattan F, Syed S, Varatharajullu P, et al.
9 Advancements in left ventricular assist devices to prevent pump thrombosis and blood
10 coagulopathy. *Journal of Anatomy* 2023;242:29–49. <https://doi.org/10.1111/joa.13675>.
- 11 [6] Kelly J, Malloy R, Knowles D. Comparison of anticoagulated versus non-anticoagulated
12 patients with intra-aortic balloon pumps. *Thrombosis Journal* 2021;19:46.
13 <https://doi.org/10.1186/s12959-021-00295-6>.
- 14 [7] James L, Kilmarx SE, Phillips K, Moazami N, Galloway AC, Eugene G, et al. CARC20: Intra-
15 operative Use of Intra-aortic Balloon Pump to Generate Pulsatile Flow During Heart
16 Transplantation. *ASAIO Journal* 2023;69:52.
17 <https://doi.org/10.1097/01.mat.0000943516.85360.f9>.
- 18 [8] González LS, Chaney MA. Intraaortic Balloon Pump Counterpulsation, Part I: History,
19 Technical Aspects, Physiologic Effects, Contraindications, Medical Applications/Outcomes.
20 *Anesth Analg* 2020;131:776–91. <https://doi.org/10.1213/ANE.0000000000004954>.
- 21 [9] Deghan Manshadi S, Eisenberg N, Montbriand J, Luk A, Roche-Nagle G. Vascular
22 Complications With Intra-aortic Balloon Pump (IABP): Experience From a Large Canadian
23 Metropolitan Centre. *CJC Open* 2022;4:989–93.
24 <https://doi.org/10.1016/j.cjco.2022.08.008>.
- 25 [10] Pelrine R, Kornbluh R, Joseph J, Heydt R, Pei Q, Chiba S. High-field deformation of
26 elastomeric dielectrics for actuators. *Materials Science and Engineering: C* 2000;11:89–
27 100. [https://doi.org/10.1016/S0928-4931\(00\)00128-4](https://doi.org/10.1016/S0928-4931(00)00128-4).
- 28 [11] Martinez T, Jahren SE, Walter A, Chavanne J, Clavica F, Ferrari L, et al. A novel soft cardiac
29 assist device based on a dielectric elastomer augmented aorta: An in vivo study.
30 *Bioengineering & Translational Medicine* 2023;8:e10396.
31 <https://doi.org/10.1002/btm2.10396>.
- 32 [12] Jahren SE, Martinez T, Walter A, Ferrari L, Clavica F, Obrist D, et al. Hemodynamic effects
33 of a dielectric elastomer augmented aorta on aortic wave intensity: An in-vivo study.
34 *Journal of Biomechanics* 2023;159:111777.
35 <https://doi.org/10.1016/j.jbiomech.2023.111777>.
- 36 [13] Wang C, Lachat M, Regar E, von Segesser LK, Maisano F, Ferrari E. Suitability of the porcine
37 aortic model for transcatheter aortic root repair. *Interact Cardiovasc Thorac Surg*
38 2018;26:1002–8. <https://doi.org/10.1093/icvts/ivx381>.

- 1 [14] Albuquerque FB, Shea H. Influence of humidity, temperature and prestretch on the
2 dielectric breakdown strength of silicone elastomer membranes for DEAs. *Smart Mater*
3 *Struct* 2020;29. <https://doi.org/10.1088/1361-665X/aba5e3>.
- 4 [15] Jiang L, Betts A, Kennedy D, Jerrams S. Eliminating electromechanical instability in
5 dielectric elastomers by employing pre-stretch. *J Phys D: Appl Phys* 2016;49:265401.
6 <https://doi.org/10.1088/0022-3727/49/26/265401>.
- 7 [16] Martinez T, Chavanne J, Walter A, Civet Y, Perriard Y. Design and modelling of a tubular
8 dielectric elastomer actuator with constrained radial displacement as a cardiac assist
9 device. *Smart Mater Struct* 2021;30:105024. <https://doi.org/10.1088/1361-665X/ac1fa8>.
- 10 [17] Lo N, Magnus Ohman E. Mechanical Circulatory Support in ST-Elevation Myocardial
11 Infarction. In: Watson TJ, Ong PJ, Tcheng JE, editors. *Primary Angioplasty: A Practical*
12 *Guide*, Singapore: Springer; 2018, p. 253–73. [https://doi.org/10.1007/978-981-13-1114-](https://doi.org/10.1007/978-981-13-1114-7_19)
13 [7_19](https://doi.org/10.1007/978-981-13-1114-7_19).
- 14 [18] Rihal CS, Naidu SS, Givertz MM, Szeto WY, Burke JA, Kapur NK, et al. 2015
15 SCAI/ACC/HFSA/STS Clinical Expert Consensus Statement on the Use of Percutaneous
16 Mechanical Circulatory Support Devices in Cardiovascular Care: Endorsed by the American
17 Heart Association, the Cardiological Society of India, and Sociedad Latino Americana de
18 Cardiologia Intervencion; Affirmation of Value by the Canadian Association
19 of Interventional Cardiology-Association Canadienne de Cardiologie d'intervention*.
20 *Journal of the American College of Cardiology* 2015;65:e7–26.
21 <https://doi.org/10.1016/j.jacc.2015.03.036>.
- 22 [19] Esposito M, Bader Y, Pedicini R, Breton C, Mullin A, Kapur NK. The role of acute circulatory
23 support in ST-segment elevation myocardial infarction complicated by cardiogenic shock.
24 *Indian Heart Journal* 2017;69:668–74. <https://doi.org/10.1016/j.ihj.2017.05.011>.
- 25 [20] Kolyva C, Pantalos GM, Giridharan GA, Pepper JR, Khir AW. Discerning aortic waves during
26 intra-aortic balloon pumping and their relation to benefits of counterpulsation in humans.
27 *Journal of Applied Physiology* 2009;107:1497–503.
28 <https://doi.org/10.1152/jappphysiol.00413.2009>.
- 29 [21] Lu P-J, Lin P-Y, Yang C-FJ, Hung C-H, Chan M-Y, Hsu T-C. Hemodynamic and metabolic
30 effects of para- versus intraaortic counterpulsatile circulation supports. *ASAIO J*
31 2011;57:19–25. <https://doi.org/10.1097/MAT.0b013e3181fcbc7d>.
- 32 [22] Meyns BP, Nishimura Y, Jashari R, Racz R, Leunens VH, Flameng WJ. Ascending versus
33 descending aortic balloon: Pumping: organ and myocardial perfusion during ischemia. *The*
34 *Annals of Thoracic Surgery* 2000;70:1264–9. [https://doi.org/10.1016/S0003-](https://doi.org/10.1016/S0003-4975(00)01703-3)
35 [4975\(00\)01703-3](https://doi.org/10.1016/S0003-4975(00)01703-3).
- 36 [23] Chyong Y, Miura I, Ramez B, Miura S, Kabei N. Aortic root balloon pumping (A.R.B.P.).
37 Experimental study and theoretical rationale. *Jpn Heart J* 1971;12:263–74.
38 <https://doi.org/10.1536/ihj.12.263>.

1 [24] Almanza M, Martinez T, Petit M, Civet Y, Perriard Y, LoBue M. Adaptation of a Solid-State
2 Marx Modulator for Electroactive Polymer. IEEE Transactions on Power Electronics
3 2022;37:13014–21. <https://doi.org/10.1109/TPEL.2022.3183437>.

4
5
6
7
8 **FIGURE LEGENDS:**

9
10 **Central Image:** New implantation of the DEA and the effect of its activation on hemodynamic
11 parameters
12

13 **Figure 1.** DEA and sensors implantation and hardware actuation and acquisition scheme. (A)
14 Schematic of the DEA design. The connectors are there to enable anastomosis with the aorta and
15 provide inner support for the DEA. The external housing helps protect the DEA from the outside
16 environment and allows to apply the pre-stretch. (B) Picture of the device before and after pre-
17 stretch is applied. The total length goes from 40 to 60 mm. (C) Schematic of the left section of
18 the heart showing the different sections of the aorta as well as the graft bypass with the DEA. (D)
19 Location of the different sensors used during the *in vivo* experiment. (E) Overview of the
20 hardware setup used during the *in vivo* experiments. The DEA is activated at high voltages (kV) in
21 synchronization with the pacing signal from the pacemaker through the CompactDAQ and the
22 LabVIEW software. HV: High Voltage PV: Pressure Volume
23

24 **Figure 2.** Description of the two different protocols for DEA actuation timing (amplitude scaled
25 to pressure) compared to the left ventricular (PLV) and aortic pressures (Pasc): (A) phase shifting
26 (PS, in % of heart cycle) where the start of the DEA actuation signal is shifted throughout the
27 heart cycle to spot the best actuation timing, (B) fine tuning where the start (S) and end (E) of the
28 activation are fine-tuned to optimize the assistance to the heart.
29

30 **Figure 3.** Overview of the impact of DEA actuation timing (ON: device on) on aortic (A-F) and left
31 ventricular (G-H) pressure parameters compared to baseline (OFF: no actuation) calculated as
32 $(100 * (\text{device-actuated} - \text{baseline}) / \text{baseline})$. (A,C,E,G) shows the impact of phase shifting
33 (protocol A) and (B, D, F, H) the impact of fine-tuning (protocol B) of the actuation timing.
34

35 **Figure 4.** Best results of (A) end-diastolic pressure ($-13 \pm 4.0\%$) and maximum aortic systolic
36 pressure ($-16 \pm 3.6\%$) decrease and (B) **mean** early aortic diastolic pressure ($10 \pm 3.5\%$) increase. (C)
37 Overall best results for all three parameters simultaneously with start of actuation at -8% of heart
38 cycle before aortic valve opening and end of actuation at 0% of heart cycle before aortic valve
39 closure.

1
2
3
4
5
6
7
8
9
10
11
12
13

Figure 5. Examples of pressure-volume curves of the left ventricle during DEA support at (A) counterpulsation compared to baseline and at (B) different actuation timings compared to baseline. Baseline: device turned off. PS: phase shift.

Figure 6. (A) Energy provided by the DEA *in vivo* and comparison between the new design using pre-stretch (E_{new}) and the older one without pre-stretch (E_{old}). With almost similar pressure conditions the new design provides more than 5 times the energy of the older design (B) Representation of one particular *in vivo* case that showcases the maximum energy provided by the DEA. The maximum energy is then of 82.3 mJ with differences of volume (ΔVol) during activation and deactivation of 3.8 mL and 28.1 mL respectively.

ACCEPTED MANUSCRIPT

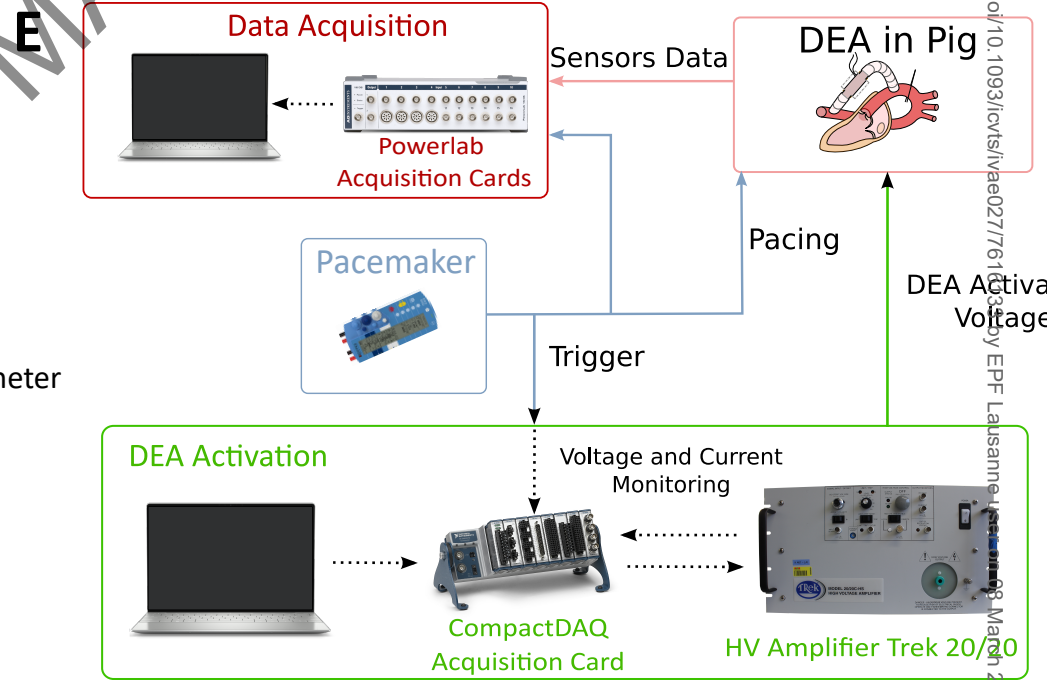
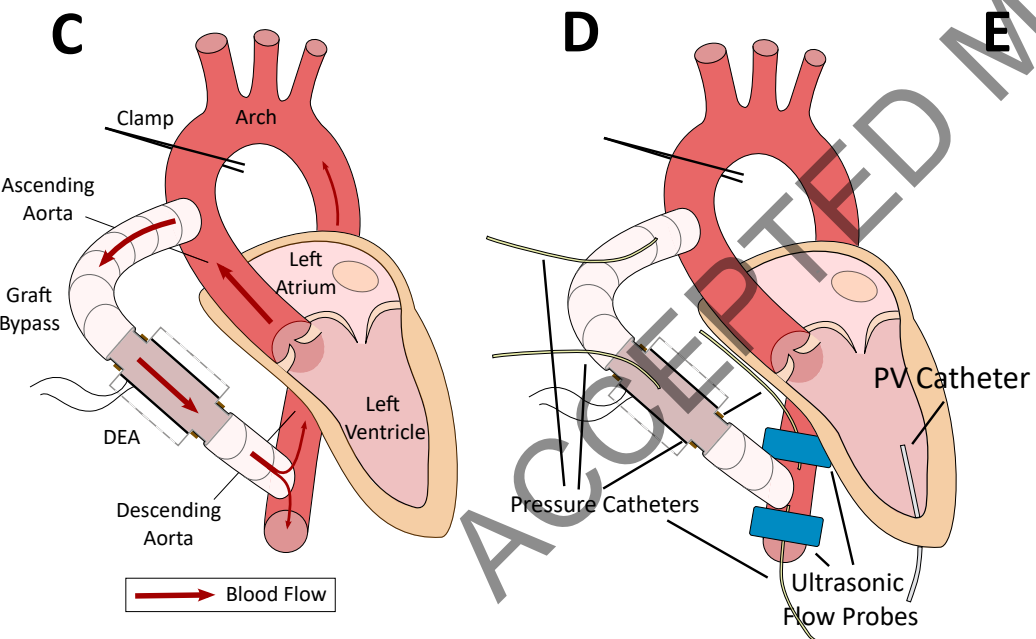
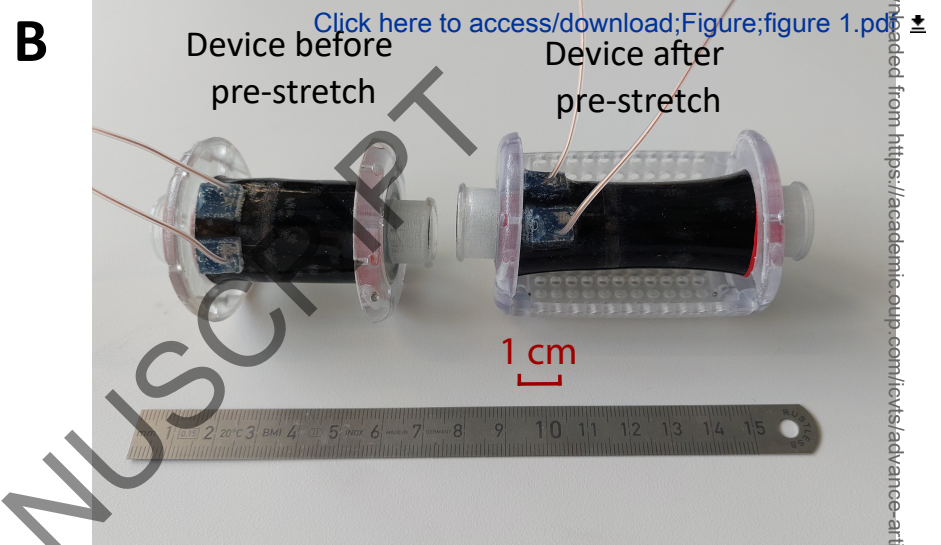
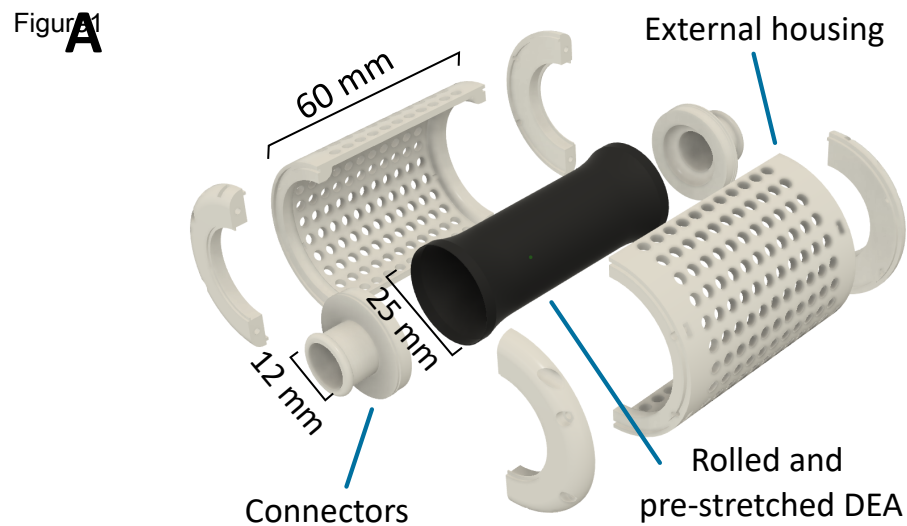
Table 1. Overview of the mean values and standard deviations of measured differences between baseline and device-actuated heart cycles ($100 \times (\text{device-actuated} - \text{baseline}) / \text{baseline}$) in the hemodynamic parameters for protocol A (phase shifting) and protocol B (fine-tuning). For each protocol, the results have been grouped in range of actuation timings (phase shifts) to showcase the optimal timing for the start (ON) and end (OFF) of DEA-actuation. Depending on which type of parameter, the actuation timing considered is either ON or OFF. For protocol A, the **mean** systolic left ventricular (LV) pressure was not included due to too few recordings with working LV pressure measurement to perform statistics.

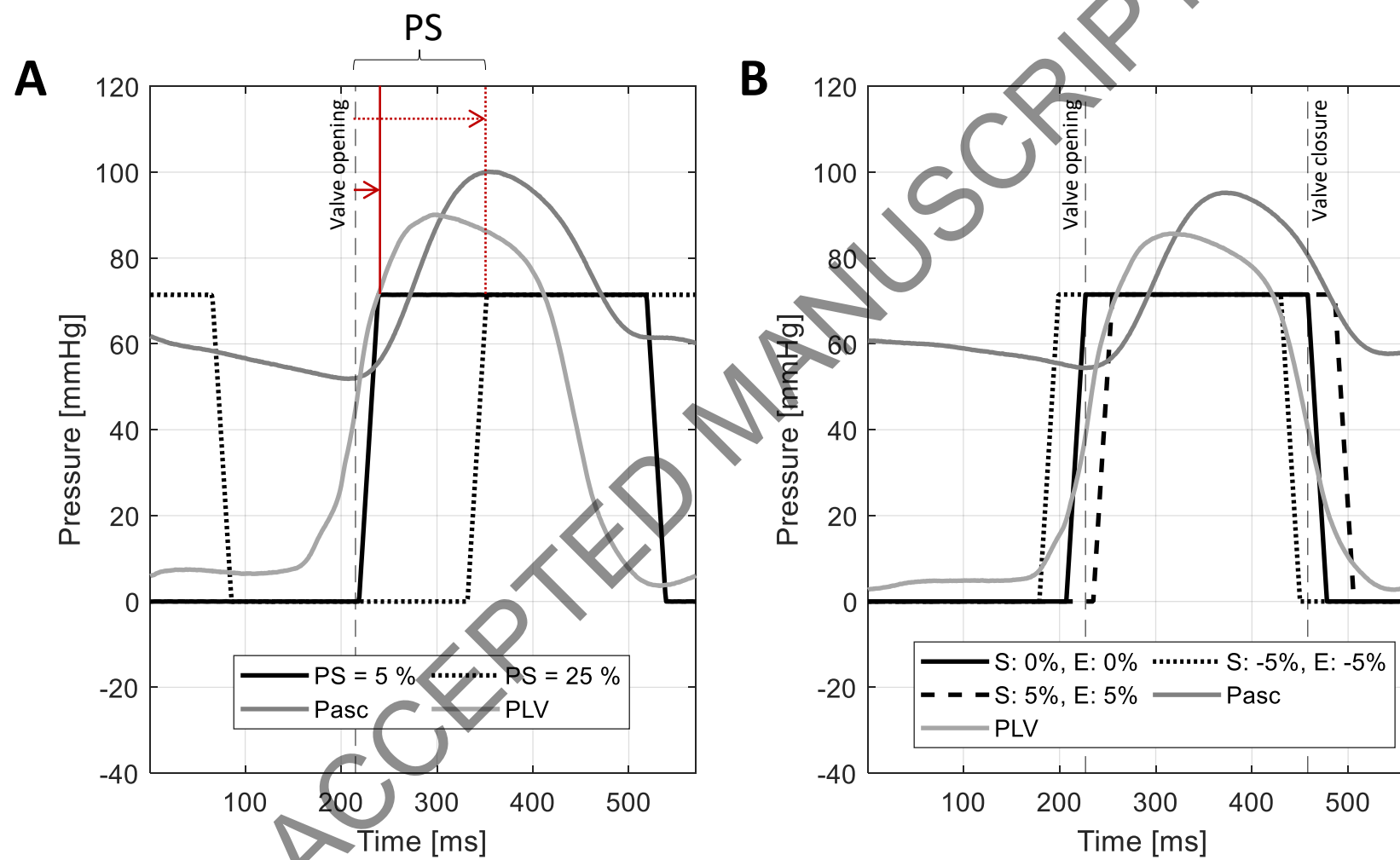
		Protocol A: phase shift									
Actuation (ON or OFF) [%]		0-10	10-20	20-30	30-40	40-50	50-60	60-70	70-80	80-90	90-100
End-diastolic pressure (ON)		1.82±2.6*	1.28±7.2*	1.65±3.0*	0.38±3.8*	4.02±4.4	-0.31±5.1*	1.27±6.3*	-3.04±1.8	-9.60±3.1	-3.57±3.2
Mean early diastolic pressure (OFF)		3.77±2.8	2.13±3.1*	-0.26±3.2*	-2.85±2.5	-4.45±1.2	-3.91±1.5	-1.43±2.3*	1.17±2.2*	3.54±2.2	4.61±2.8
Maximum systolic pressure (ON)		-5.48±4.0	-6.68±3.6	-2.66±2.5	0.95±1.1	0.34±1.3*	0.56±1.2*	0.81±2.3*	3.65±3.4*	3.23±3.5	-3.02±1.5

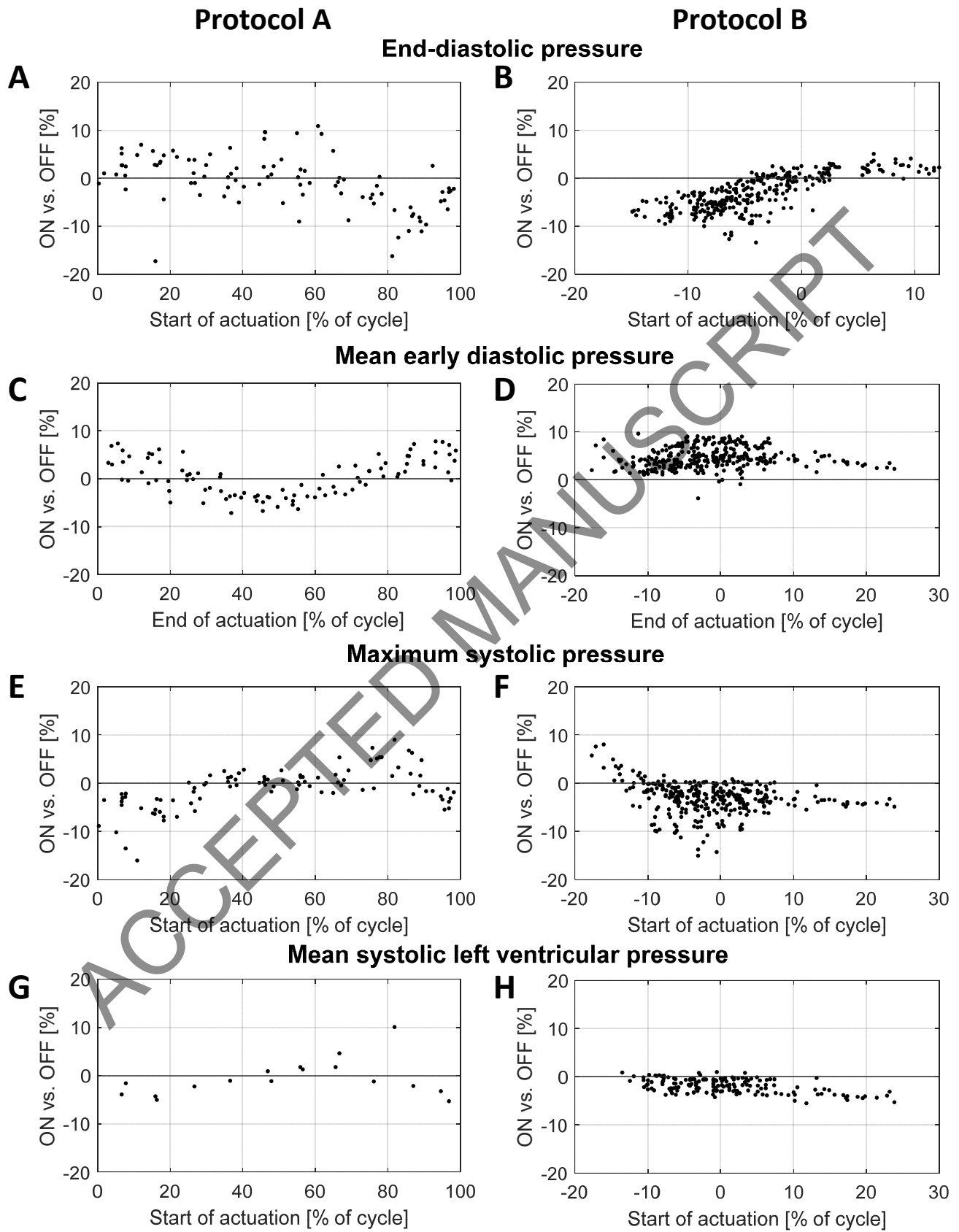
		Protocol B: fine-tuning				
Actuation (ON or OFF) [%]		-15-10	-10-5	-5-0	0-5	5-10
End-diastolic pressure (ON)		-6.60±1.7	-5.25±2.4	-2.05±3.1	0.82±1.9	2.32±1.2
Mean early diastolic pressure (OFF)		3.64±2.1	4.16±1.8	4.94±2.5	5.31±2.2	5.19±1.8
Maximum systolic pressure (ON)		-2.51±2.2	-2.23±2.7	-3.24±3.1	-3.21±3.6	-6.36±3.9
Mean systolic LV pressure (ON)		-0.81±1.1*	-1.22±1.2	-2.42±1.2	-2.48±1.3	-3.52±1.5

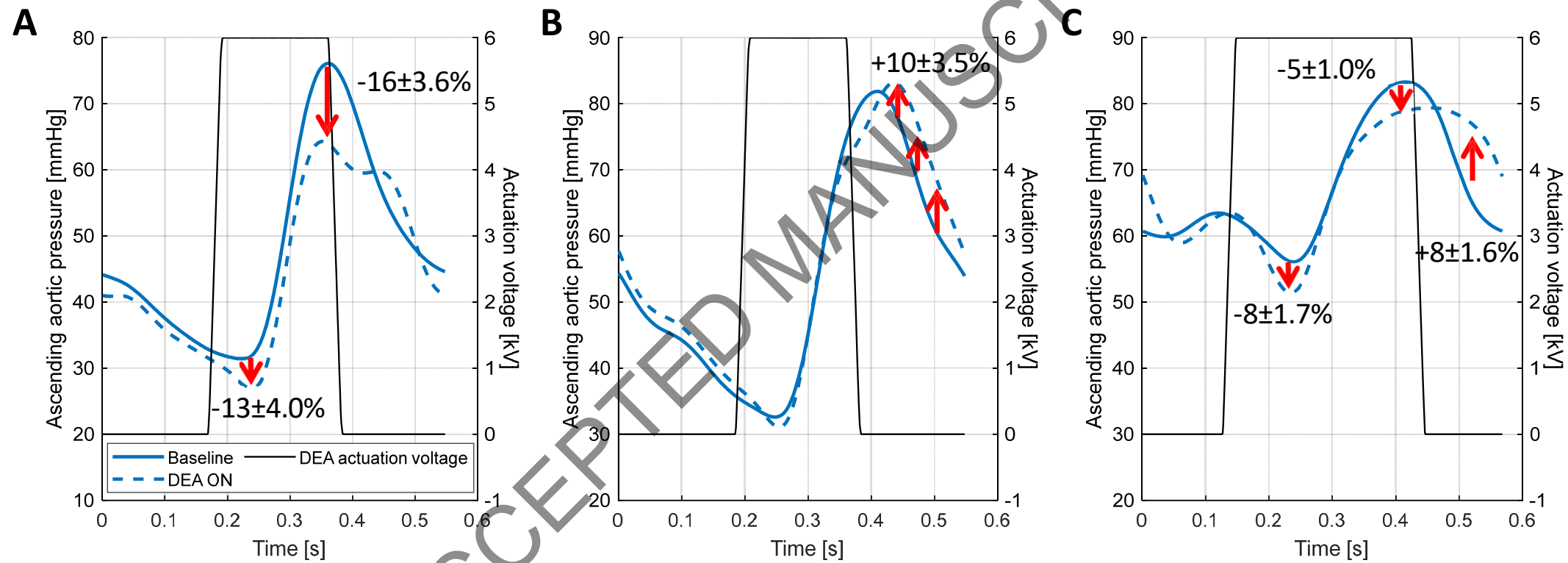
*non-significant change

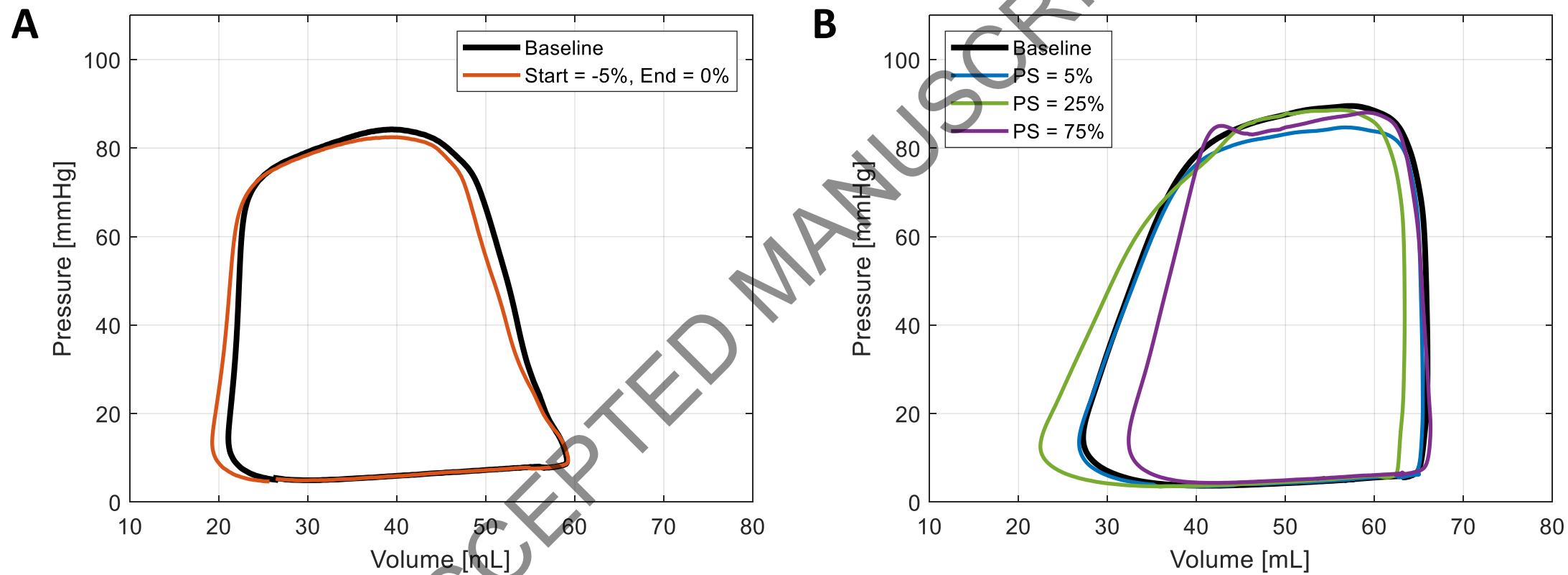
LV: left ventricular

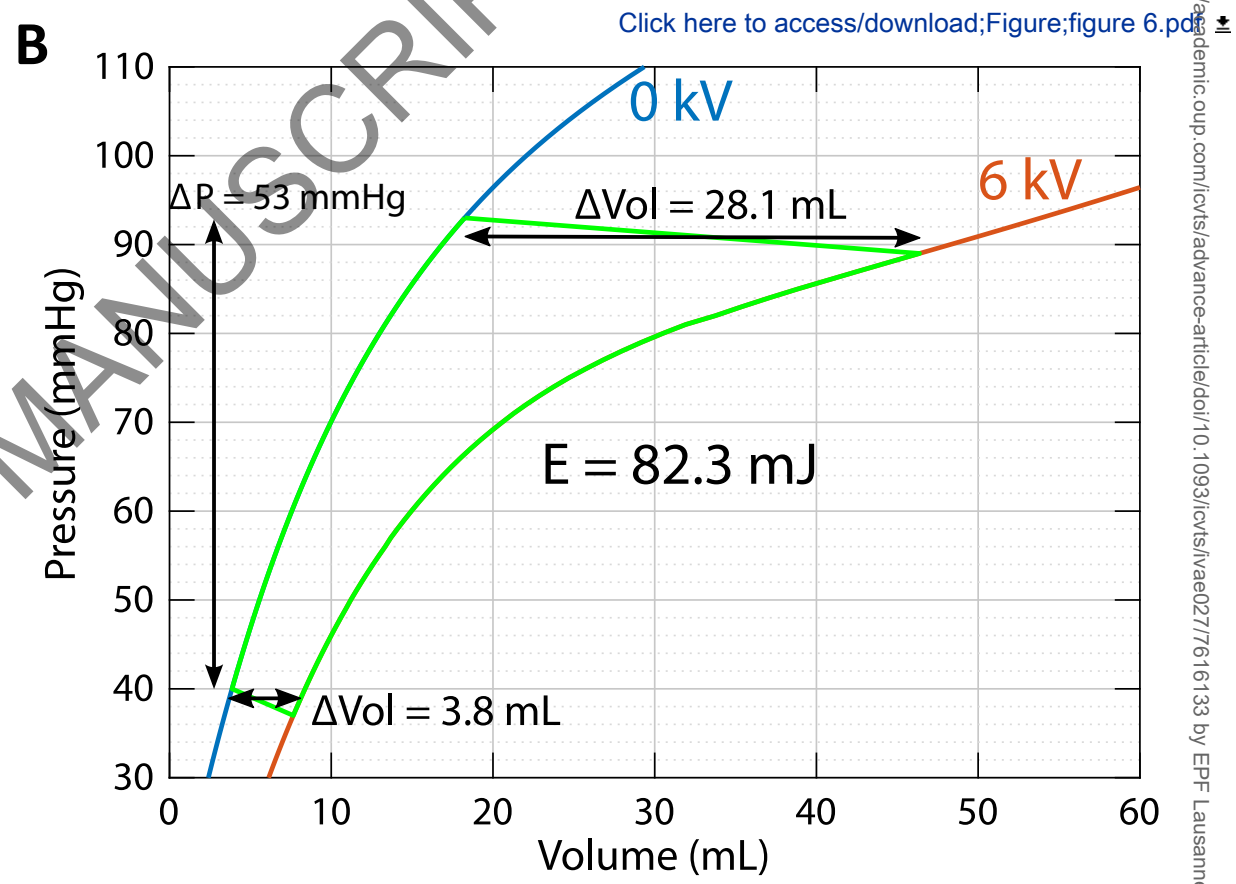
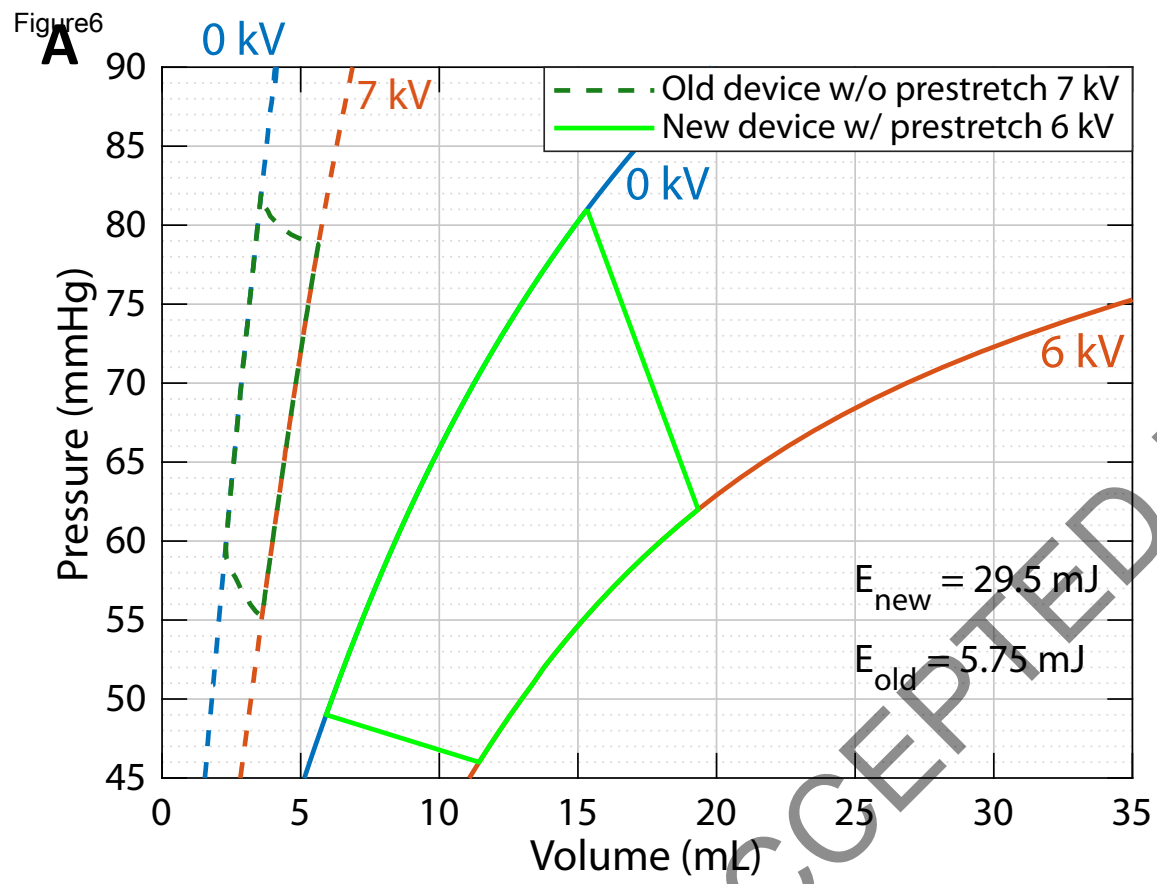










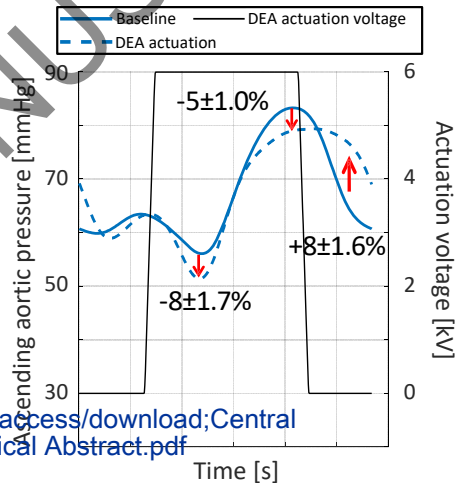


Novel para-aortic assistance using pre-stretched dielectric elastomer actuator

Summary

A new pre-stretched dielectric elastomer actuator (DEA) cardiac assist device was implanted in 2 pigs to act as a counter-pulsation system.

We compare the pressure in the ascending aorta during baseline and during actuation of the device to assess the impact of the device. The proposed system helps to reduce the end-diastolic pressure and peak systolic pressure as well as increases the average diastolic pressure.



[Click here to access/download;Central image;Graphical Abstract.pdf](https://academic.oup.com/central-image/Graphical-Abstract.pdf)

Legend: New implantation of the DEA and its effect on the hemodynamic parameters